

High-spin structure of $N = 51$ ^{96}Rh and ^{97}Pd : A shell-model study

W. F. Piel, Jr., D. B. Fossan, R. Ma, E. S. Paul, and N. Xu

Physics Department, State University of New York at Stony Brook, Stony Brook, New York 11794

J. B. McGrory

Physics Division, Oak Ridge National Laboratory, Oak Ridge, Tennessee 37831

(Received 10 October 1989)

High-spin states of isotonic ^{96}Rh and ^{97}Pd were studied by means of the $^{64}\text{Zn}(^{40}\text{Ca}, \alpha 3pn \gamma)^{96}\text{Rh}$ and $^{64}\text{Zn}(^{40}\text{Ca}, \alpha 2pn \gamma)^{97}\text{Pd}$ reactions, respectively, with $E_{\text{lab}} = 167$ MeV. Levels up to 5.5 MeV with $J^\pi = 15^+$ in ^{96}Rh were populated while levels in ^{97}Pd up to 7.5 MeV were found. The yrast $\frac{21}{2}^+$ level of ^{97}Pd was found to decay to a $\frac{19}{2}^+$ level, in contrast to the behavior of the lighter odd- A isotones. An attempt to measure lifetimes using a neutron- γ coincidence technique revealed no new isomers in either nuclide with $t_{1/2} \geq 5$ ns. The discovery of two low-lying transitions of 125 keV in ^{96}Rh requires a slight revision of a recently reported value of its atomic mass as well as that of isobaric ^{96}Pd . The high-spin structure and the $N = 51$ systematics, particularly the location of the $vg_{7/2}$ strength, are compared with the results of shell-model calculations.

I. INTRODUCTION

The investigation of nuclei with one particle outside of a closed shell has been, over the years, a fruitful confrontation between theory and experiment. The present empirical results for two nuclei, each with 51 neutrons, can be compared to the results of shell-model calculations. These calculations have typically considered the coupling of a $d_{5/2}$ neutron to $g_{9/2}$ protons (or proton holes) outside of a ^{88}Sr (^{100}Sn) core. The new data for the $N = 51$ nuclei complements recent reports from this and other laboratories¹⁻⁶ of new data for both the $N = 50$ and the $N = 52$ systems. These previous reports emphasized either a search for collective $vg_{9/2}^{-1}$ intruder bands, a test of seniority conservation for $g_{9/2}$ protons, or a study of how collective excitations are built up as one adds valence particles to closed shells. In the present study, we have three goals in mind. A study of odd-odd ^{96}Rh can be expected to shed light on the residual proton-neutron interaction. Second, since these are the heaviest $N = 51$ nuclides hitherto studied, the $\pi g_{9/2} \nu g_{9/2}$ overlap is larger, which might induce measureable high-spin isomers. Finally, one is interested in locating the $vg_{7/2}$ strength, e.g., the strength contained in the yrast $\frac{7}{2}^+$ level. This strength apparently is not important in the high-spin structure of the lighter isotones but has finally become low-lying in the spectrum of ^{97}Pd . The location of the $vg_{7/2}$ strength throughout this mass region is of current interest in regard to the quenching of Gamow-Teller strength during beta decays of the type $\pi g_{9/2} \rightarrow \nu g_{7/2}$.

The only previous empirical information on the excited states of ^{96}Rh has come from studies of the $\beta^+ + \text{EC}$ decay of ^{96}Pd . The most recent study by Rykaczewski *et al.*⁷ located four low-lying 1^+ states, and two other states, in addition to the two beta-decaying isomers of ^{96}Rh . The two isomers were tentatively proposed to have

$J^\pi = (3)^+$ and $(6)^+$, with the $(3)^+$ level located 52.0 keV above the $(6)^+$ level. For ^{97}Pd , a previous study by Fettweis *et al.*,⁸ who used the $^{96}\text{Ru}(^3\text{He}, 2n \gamma)$ reaction with $E_{\text{lab}} = 20$ MeV has located medium-spin states up to 2.5 MeV. The lower-lying states found in the present work are in agreement with the previous results as will be shown. Finally, a preliminary report of the present work has appeared⁹ as well as a shell-model calculation¹⁰ of the energies of the ^{96}Rh levels.

II. EXPERIMENTS

The $^{64}\text{Zn}(^{40}\text{Ca}, \alpha 3pn \gamma)^{96}\text{Rh}$ and $^{64}\text{Zn}(^{40}\text{Ca}, \alpha 2pn \gamma)^{97}\text{Pd}$ reactions with $E_{\text{lab}} = 167$ MeV were used to study ^{96}Rh and ^{97}Pd using ^{40}Ca ions produced by the Stony Brook linear accelerator (LINAC). The ^{64}Zn target of 1.1 mg/cm² was enriched to 99.5% and backed by 35 mg/cm² of lead to stop the beam. The data reported here include γ -ray excitation functions, angular distributions, neutron- γ -ray coincidences, neutron- γ -ray time-delay distributions and γ - γ coincidences. The last set of data was recorded using four 25%, measured with respect to a 7.6 by 7.6 cm NaI(Tl) detector for 1.33 MeV γ rays, germanium detectors, each with a bismuth germanate anti-Compton shield of the transverse type.¹¹ These data have already been utilized to report⁴ new states of ^{99}Ag and ^{100}Cd . That paper may be consulted for additional details about the experimental techniques.

III. RESULTS

A γ -ray singles spectrum produced by $^{40}\text{Ca} + ^{64}\text{Zn}$ with $E_{\text{lab}} = 167$ MeV shows the production of several residual nuclei and appears in Fig. 1 of Ref. 4. Moreover, a spectrum gated by one neutron appears in Fig. 3(b) of Ref. 4 and displays several strong transitions in both ^{96}Rh and ^{97}Pd . The first assignment of six transitions to ^{96}Rh was also considered in Figs. 3 and 8 of Ref. 1. This assign-

ment was partly based on the observation of intensity ratios in proton-gated spectra. The energies of the six transitions (in keV) are 99.8, 125.6, 156.9, 526.7, 626.7, and 1267.1. Gamma-gamma coincidence gates were set on the strongest transitions in each nuclide and the event-mode-recorded magnetic tapes were scanned to produce background-subtracted gated spectra. Additional transitions in each nucleus could then be identified and gated on; this process continued in an iterative manner until no additional transitions could be found in the spectra. Fig. 1(b) shows the summed spectrum of seven ^{96}Rh gates that are largely free of contaminating transitions in other nuclei. The level scheme that has been constructed from the γ - γ coincidence data is presented in Fig. 2. Similarly for ^{97}Pd , the sum spectrum of six gates is given in Fig. 1(a), while the proposed ^{97}Pd level scheme is displayed in Fig. 3.

In order to obtain information about the multipolarity of each transition, the formula

$$W(\theta) = A_0 + A_2 P_2[\cos(\theta)] + A_4 P_4[\cos(\theta)] \quad (1)$$

was fitted to the observed γ -ray intensity function $W(\theta)$, where θ is the angle of the detector measured with respect to the beam direction. The data were simultaneously recorded in two modes, namely, both singles and neutron gated, as described in Ref. 4. The data taken in singles mode offered superior statistical accuracy, while the neutron-gated data were less contaminated by transitions in other nuclei. The angular distribution results for ^{96}Rh and ^{97}Pd are summarized in Tables I and II, respectively. For several $\Delta I = 1$ transitions, the $E2/M1$ mixing ratios could be determined. The uncertainties listed in Tables I and II for these take into account the uncertainty in determining the alignment parameters α_2 and α_4 . The spin and parity assignments proposed in Figs. 2 and 3 are based both on the angular distribution results and on the $N = 51$ systematics.

A. ^{96}Rh Level scheme

The two beta-decaying isomers of ^{96}Rh shown in Fig. 2 have tentatively been assigned⁷ $J^\pi = 3^+$ and 6^+ for the

first excited and ground states, respectively. The high-spin isomer apparently does not directly populate the 4^+ level of the ^{96}Ru daughter nucleus. Although the absence of beta feeding is not a strong argument for making spin-parity assignments, the 6^+ assignment should nevertheless be considered more likely than, say, a 5^+ one. The connecting 52.0 keV isomeric transition has been given an $M3$ assignment based on a measurement¹² of the K shell internal conversion coefficient $\alpha_K = 350 \pm 90$. Taking into account the branching intensity of $60\% \pm 5\%$ and the half-life¹² of 1.51 ± 0.02 min, the $B(M3)$ value would be 1.4 Weisskopf unit (W.u.) if the $E4$ contribution is not significant. This result is in the range of other $B(M3)$ values in this mass region. The transition cannot be predominantly $E4$ both because the theoretical value¹³ $\alpha_K(E4) = 532$ is larger than the empirical one and because the half-life would be much longer (the $E4$ single proton estimate is $t_{1/2}^{sp} = 0.38$ y).

The separate group of five low-spin levels shown to the left in Fig. 2 was seen more definitively in beta-decay work⁷ and are included here in order to give a rather complete picture of ^{96}Rh . In addition to these five levels, two additional higher lying $J^\pi = 1^+$ states were found.⁷ The present data are not sensitive enough to infer these additional two levels.

The most intense transition shown in Fig. 2 has an energy of 125.6 keV and is assumed to populate the ground state. This transition is distinct from the unresolved 124.7 keV transition found⁷ from the beta decay of ^{96}Pd . This was verified by setting γ - γ coincidence gates on transitions in both parts of Fig. 2 and observing a definite shift in the transition energy as listed in Table I. The 125.6 keV transition is seen to have a negative A_2/A_0 value and is assigned to be a $7^+ \rightarrow 6^+$ transition between the two highest-spin members of the

$$\pi p_{1/2}^2 g_{9/2}^5 (\nu=1) v d_{5/2}$$

multiplet. The 3^+ and $(2)^+$ levels at 52.0 and 176.7 keV excitation, respectively, are likely two other members of this multiplet. The spin-parity assignments shown in Fig.

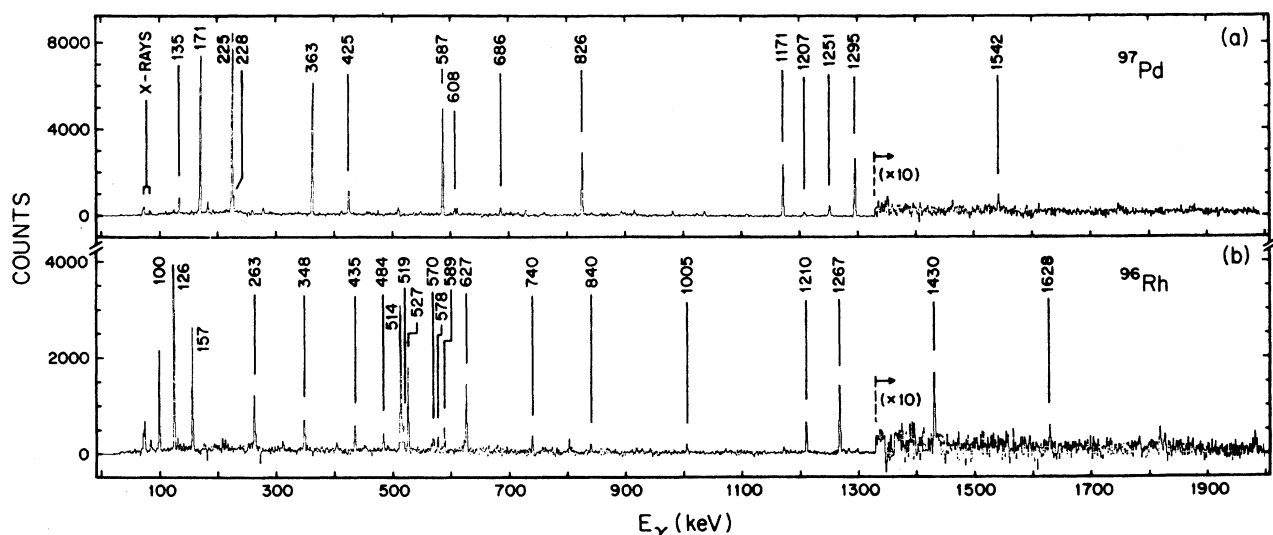


FIG. 1. (a) Sum spectrum of six background-subtracted coincidence gates set on the ^{97}Pd transitions (in keV): 170.7, 224.8, 362.5, 586.9, 899.0, and 982.0. (b) Similarly for seven ^{96}Rh transitions: 99.8, 125.6, 404.3, 526.7, 577.5, 1210.2, and 1267.1.

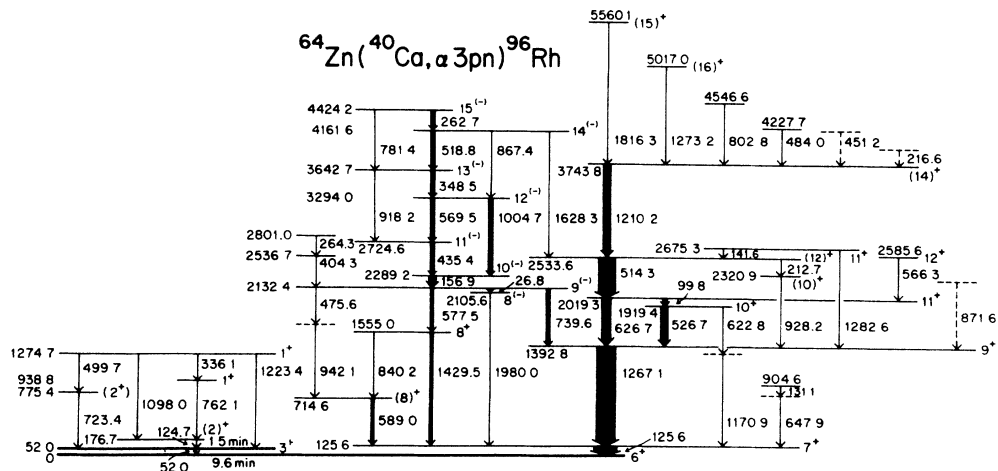


FIG. 2. The proposed level scheme for ^{96}Rh . The widths of the arrows indicate γ -ray intensities, while the energies are indicated in units of keV. The separate group of low-spin levels shown to the left were identified more definitively in studies (Ref. 7) of the $\beta^+ + \text{EC}$ decay of ^{96}Pd , which also found two additional high lying 1^+ states (not shown). The two beta-decaying isomers are each indicated by a heavy horizontal line. The 26.8 keV transition reported here was not directly observed but was inferred from γ - γ coincidence results, as discussed in the text.

2 are based on the tentative assignment⁷ of 6^+ for the ground state. A consequence of the observation of two low-lying transitions near 125 keV for the currently accepted values of the atomic masses of ^{96}Rh and ^{96}Pd is discussed later.

The 1267.1 keV transition is the most intense transition feeding the 7^+ level. This transition has a positive

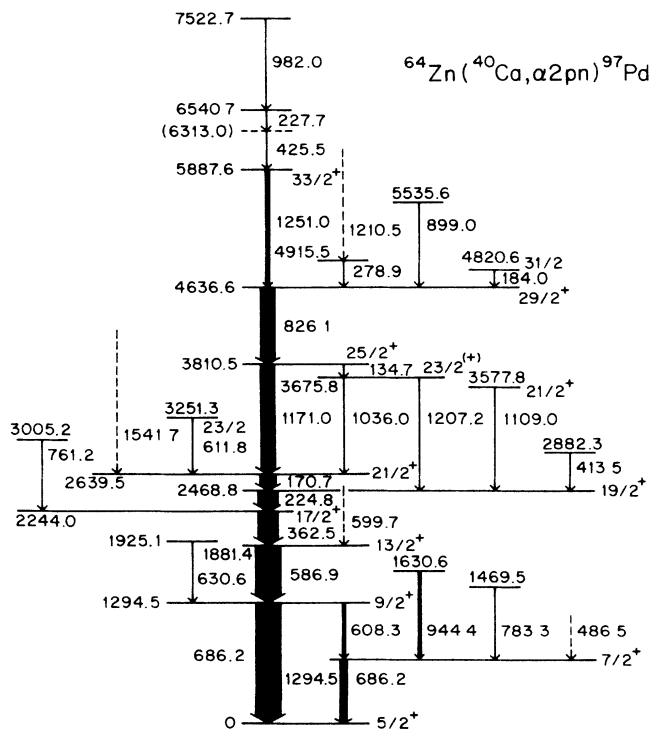


FIG. 3. The proposed level scheme for ^{97}Pd . The widths of the arrows indicate γ -ray intensities, while the energies are given in units of keV. Four additional levels of medium spin below 2.5 MeV (not shown) have been reported (Ref. 8) from ($^3\text{He}, 2n\gamma$) data.

A_2/A_0 value and is assigned to be a stretched $E2$ transition. The 1392.8 keV level is populated by the two intense transitions of 526.7 and 626.7 keV. The A_2/A_0 value for the first transition is large and negative, indicating an $M1/E2$ transition from a 10^+ state. The second transition is problematic since it was unresolved from a transition in ^{100}Ag , which is nearly half as intense. However, the A_2/A_0 value of -0.04 ± 0.09 listed in Table I for the 99.8 keV transition indicates that the 2019.3 keV level has $J^\pi = 10^+$ or 11^+ . In the isotope ^{94}Tc , an $11^+ \rightarrow 9^+$ transition of 690 keV was found¹⁴ from the $(\alpha, 3n\gamma)$ reaction. This transition is related to a $17/2^+ \rightarrow 13/2^+$ transition of 750 keV in the $N=50$ core nucleus ^{93}Tc by the coupling of a $d_{5/2}$ neutron to the maximum possible spin. We propose that the 626.7 keV transition in ^{96}Rh is similarly related to a 716 keV $17/2^+ \rightarrow 13/2^+$ transition found¹⁵ in ^{95}Rh . Therefore, the 2019.3 keV level of ^{96}Rh is assigned $J^\pi = 11^+$, which is in agreement with the positive A_2/A_0 value found for the 626.7 keV transition, i.e., it is a stretched $E2$ transition. The 2533.6 keV level can be assigned either 12^+ or 13^+ . However, there are difficulties with either assignment and we tentatively indicate a 12^+ assignment in Fig. 2. Then, the 3743.8 keV level is probably 14^+ , based on an $E2$ assignment for the 1210.2 keV transition.

The 26.8 keV transition shown in Fig. 2 was not observed but was inferred from the observation that the 1980.0 keV transition is in coincidence both with transitions feeding the 2132.4 keV level and with the strong 125.6 keV transition. This result implies that the 26.8 keV transition involves a spin change of 0 or 1, since otherwise the lifetime of the level emitting the transition would be too long to yield coincidences ($2\tau = 100$ ns). The negative A_2/A_0 value found for the 1980.0 keV transition is consistent with a dipole assignment. Then the intermediate level has $J=8$. If the 26.8 keV transition were to follow the 1980.0 keV one, then a $J=8$ level at 152 keV would be implied. This result is not support-

TABLE I. Transitions in ^{96}Rh produced by 167 MeV $^{40}\text{Ca} + ^{64}\text{Zn}$. The relative γ -ray intensities and angular distribution results are obtained from neutron-gated spectra and have been corrected for the efficiency and finite size of the detector. Several of the weaker transitions have been fitted by assuming that $A_4=0$. The $E2/M1$ mixing ratios δ are listed, using the phase convention of Yamazaki (Ref. 16), for four transitions.

E_γ (keV)	I_γ	A_2/A_0	A_4/A_0	Assignment
26.8				$9^{(-)} \rightarrow 8^{(-)}$
99.82(15)	$\sim 23^b$	$-0.04(9)^b$	$+0.11(16)^b$	$11^+ \rightarrow 10^+$
124.70(35)	a	a	a	$(2)^+ \rightarrow 3^+$
125.62(15)	$\sim 123^b$	$-0.19(5)$	$+0.08(10)$	$7^+ \rightarrow 6^+$
131.10(35)	$4.0(6)^b$	$-0.59(30)$	$\equiv 0$	$(905 \rightarrow)$
141.61(25)	$1.2(3)^c$	-	-	$11_2^+ \rightarrow (12)^+$
156.88(15)	$30.6(3.5)^c$	$-0.19(8)$	$-0.13(15)$	$10^{(-)} \rightarrow 9^{(-)}$
212.72(20)	$1.4(7)^c$	a	a	$(12)^+ \rightarrow (10_2)^+$
216.56(30)	$1.6(5)^c$	a	a	$(\rightarrow 14^+)$
262.74(30)	$20.7(3.5)^c$	a	a	$15^{(-)} \rightarrow 14^{(-)}$
264.34(30)	$3.7(1.0)^c$	a	a	$2801 \rightarrow 2537$
336.1				$1_2^+ \rightarrow 1_1^+$
348.53(25)	$19.8(1.1)^c$	$-0.52(8)^{b,d}$	$-0.17(15)^{b,d}$	$13^{(-)} \rightarrow 12^{(-)}$
				$-0.36 \leq \delta \leq -0.11$
404.30(25)	$5.7(8)$	$+0.41(48)$	$\equiv 0$	$2537 \rightarrow 9^{(-)}$
435.36(25)	$18.9(1.1)$	$-0.37(17)$	$-0.11(30)$	$11^{(-)} \rightarrow 10^{(-)}$
				$-0.34 \leq \delta \leq +0.06^e$
451.17(45)	$3.6(1.2)$	$-0.09(43)$	$\equiv 0$	$(\rightarrow 14^+)$
475.56(20)	$3.7(5)^c$	a	a	$(9^- \rightarrow)$
483.96(30)	$6.7(9)^c$	a	a	$4228 \rightarrow (14)^+$
499.7				$1_2^+ \rightarrow (2_2^+)$
514.30(20)	$74(3)$	$+0.24(6)$	$-0.21(12)$	$(12)^+ \rightarrow 11^+$
518.75(25)	$15.4(1.2)^c$	$-0.26(28)^d$	$\equiv 0$	$14^{(-)} \rightarrow 13^{(-)}$
526.72(20)	$34.9(9)^b$	$-0.38(7)^b$	$-0.00(14)^b$	$10^+ \rightarrow 9^+$
				$-0.22 \leq \delta \leq -0.022$

ed by the shell-model calculations presented later. Therefore, it is assumed that the 26.8 keV transition precedes the higher-energy one, implying a $J=8$ level at 2105.6 keV.

The 714.6 keV level is depopulated by the 589.0 keV transition. Since no transition to the ground state could be found, the possibilities are that $J^\pi=8^+$, 8^- , or 9^+ . The possibility of 9^- can be ruled out since in that case the resulting $M2$ transition would have had an observable half-life. Such a half-life was not observed as discussed later. Moreover, the choice of 8^- can be ruled out since the empirical A_2/A_0 value is positive. The data do not allow a definite choice to be made between 8^+ and 9^+ , and we tentatively indicate $(8)^+$ in Fig. 2.

The 2132.4 keV level is depopulated mainly by the 577.5 and 739.6 keV transitions. Since no transition to the 7^+ level was seen, an assignment of 8^+ can be ruled out. An 8^- assignment can also be ruled out since, in that case, the A_2/A_0 value for the 739.6 keV transition would be negative, in contrast to experiment. The spin cannot be greater than nine since the A_2/A_0 value for the 1980.0 keV transition is negative. This leaves the possibilities 9^+ or 9^- . The level is tentatively assigned to be $9^{(-)}$.

The 1555.0 keV level is fed by the 577.5 keV transition and is depopulated mainly by the 1429.5 keV transition. The possible J^π values are 8^+ , 8^- , or 9^- . The 8^- assignment can be ruled out since the A_2/A_0 value for the

1429.5 keV transition would be negative, in disagreement with experiment. A spin of nine can be ruled out since, in that case, the A_4/A_0 value for the 577.5 keV transition would be large and negative, in contrast to experiment. Therefore, $J^\pi=8^+$ is assigned to the 1555.0 keV level.

The 2289.2 keV level is assigned $J^\pi=10^{(-)}$. The structure of this level may be

$$\pi p_{1/2}^2 g_{9/2}^5 (\nu=1) \nu h_{11/2}$$

The nine transitions above this level appear to be $M1$ and $E2$ crossover transitions. This result yields assignments of 11^- to 15^- for the five levels that are involved. The four $E2$ transition energies are seen to decrease as the spin increases. The 1628.3 keV transition connects the 4161.6 and 2533.6 keV levels and has a positive value for A_2/A_0 . Assuming that these two levels have opposite parity, then this is likely a stretched $M2$ transition $14^{(-)} \rightarrow (12)^+$.

B. ^{97}Pd Level scheme

The excited medium spin levels of ^{97}Pd shown in Fig. 3, which were also found⁸ from the $(^3\text{He}, 2n\gamma)$ reaction and assigned spin-parities are $\frac{7}{2}^+$, $\frac{9}{2}^+$, $\frac{13}{2}^+$, and $\frac{17}{2}^+$. In addition, the 2468.8 keV level was inferred but the spin was not assigned. Four additional levels, not reported here, were also found: 1942.3 ($\frac{11}{2}^+$), 2140.3, 2175.4, and 2480.7 keV.

TABLE I. (Continued).

E_γ (keV)	I_γ	A_2/A_0	A_4/A_0	Assignment
566.32(35)	7.9(1.1)	-0.82(33)	$\equiv 0$	$12_2^+ \rightarrow 11^+$
569.52(35)	11.5(1.1) ^c	a	a	$12^{(-)} \rightarrow 11^{(-)}$
577.52(30)	14.7(1.9) ^c	-0.16(13) ^b	+0.32(22) ^b	$9^{(-)} \rightarrow 8_2^+$
589.01(35)	15.2(9) ^c	+0.28(15)	$\equiv 0$	$(8)^+ \rightarrow 7^+$
622.83(25)	4.5(1.1) ^c	a	a	$(10^+ \rightarrow)$
626.70(20)	48(3) ^c	+0.20(10) ^{b,d}	-0.08(10) ^{b,d}	$11^+ \rightarrow 9^+$
647.89(45)	4.3(1.2) ^c	a	a	$(\rightarrow 7^+)$
723.4				$(2_2^+) \rightarrow 3^+$
739.65(30)	20.5(2.8)	+0.49(21)	+0.78(35)	$9^{(-)} \rightarrow 9^+$
762.14(30)				$1^+ \rightarrow (2)^+$
781.44(25)	4.9(6) ^c	a	a	$15^{(-)} \rightarrow 13^{(-)}$
802.83(35)	6.1(1.3) ^c	a	a	$4547 \rightarrow (14)^+$
840.21(30)	5.9(8) ^c	+0.14(27)	$\equiv 0$	$8_2^+ \rightarrow (8)^+$
867.40(35)	2.7(7) ^c	a	a	$14^{(-)} \rightarrow 12^{(-)}$
871.60(45)	5.8(2.8) ^c	a	a	$(\rightarrow 9^+)$
918.18(30)	6.6(7) ^c	+0.27(34) ^d	$\equiv 0$	$13^{(-)} \rightarrow 11^{(-)}$
928.18(35)	7.1(8)	-0.14(26)	$\equiv 0$	$(10_2)^+ \rightarrow 9^+$
942.07(35)	4.6(9) ^c	a	a	$(\rightarrow 8^+)$
974.66(35)	1.9(7) ^c	a	a	^{96}Rh
1004.72(20)	14.0(3.6) ^c	a	a	$12^{(-)} \rightarrow 10^{(-)}$
1098.01(30)				$1_2^+ \rightarrow (2)^+$
1170.88(30)	7.2(8) ^c	a	a	$(\rightarrow 7^+)$
1210.17(20)	41(2) ^c	+0.22(12) ^d	+0.02(21) ^d	$(14)^+ \rightarrow (12)^+$
1223.4				$1_2^+ \rightarrow 3^+$
1267.13(20)	$\equiv 100.0(1.8)^b$	+0.29(6) ^b	+0.03(10) ^b	$9^+ \rightarrow 7^+$
1273.24(30)	3.2(8) ^c	+0.71(44) ^d	$\equiv 0$	$(16)^+ \rightarrow (14)^+$
1282.64(35)	3.6(1.3) ^c	a	a	$11_2^+ \rightarrow 9^+$
1429.53(25)	11.5(1.4)	+0.67(30)	$\equiv 0$	$8_2^+ \rightarrow 7^+$
				+0.31 $\leq \delta \leq$ +5.1
1628.32(20)	4.0(1.2) ^c	+0.23(17) ^b	$\equiv 0$	$14^{(-)} \rightarrow (12)^+$
1816.27(25)	5.3(1.0) ^b	-0.23(28) ^b	$\equiv 0$	$(15)^+ \rightarrow (14)^+$
1979.97(30)	5.9(7) ^c	-0.27(27) ^b	$\equiv 0$	$8^{(-)} \rightarrow 7^+$

^aTransition is unresolved from another.

^bValue obtained from spectra recorded in singles mode.

^cValue obtained from γ - γ coincidence spectra.

^dValue may be perturbed by an unresolved transition.

^eThere is also a solution with $|\delta| > 1$.

The 224.8 keV transition that depopulates the 2468.8 keV level has a negative A_2/A_0 ratio as is listed in Table II. Therefore, this level can be assigned a spin of $\frac{19}{2}$. We discuss the parity assignment for this level further. The 170.7 keV transition has $A_2/A_0 = -0.29 \pm 0.03$. This value appears to be different from the value of -0.189 ± 0.032 expected for a stretched dipole transition. This expectation is based on an alignment parameter¹⁶ $\alpha_2 = 0.66 \pm 0.11$, which is the average value for the $\frac{17}{2}^+ \rightarrow \frac{13}{2}^+$ and $\frac{13}{2}^+ \rightarrow \frac{9}{2}^+$ $E2$ transitions. Therefore, the 170.7 keV transition is an $M1/E2$ mixture and the $\frac{21}{2}$ and $\frac{19}{2}$ levels have the same parity. Moreover, no $\frac{21}{2} \rightarrow \frac{17}{2}^+$ transition could be found in the data and the empirical upper limit for the intensity is 1.0 [$I_\gamma(1294.5) \equiv 100$]. Shell-model calculations presented later predict an intensity of 0.27 for a $\frac{21}{2}^+ \rightarrow \frac{17}{2}^+$ transition. This value is seen to be in agreement with the

empirical upper limit. The yrast $J = \frac{21}{2}$ levels found in the lighter odd- A isotones have been assigned positive parity. Moreover, the prediction of the shell-model calculations presented later is that the yrast $\frac{21}{2}$ level in ^{97}Pd also has positive parity. Therefore, we assign $\frac{21}{2}^+$ to the 2639.5 keV level. The decay of the $\frac{21}{2}^+$ level is different from the lighter odd- A isotones that were found to decay either by a $\frac{21}{2}^+ \rightarrow \frac{17}{2}^+$ $E2$ transition (^{95}Ru and ^{91}Zr) or by a $\frac{21}{2}^+ \rightarrow \frac{13}{2}^+$ $E4$ isomeric transition (^{93}Mo).

The 3810.5 keV level depopulates mainly by the 1171.0 keV transition. Although this transition is unresolved from a transition in ^{100}Ag that is 34% as intense, the angular distribution results are consistent with a stretched $E2$ assignment. Similarly, the results for the 826.1 and 1251.0 keV transitions suggest stretched $E1$ assignments.

A search for new isomeric levels was made by recording the time delays between fast neutrons striking any

one of four detectors utilizing NE213 liquid scintillator and γ rays striking a germanium detector. The time resolution, with the neutron detectors located 10 cm downstream from the target, was 20 ns full width at half maximum (FWHM). No new isomer with a half-life longer than 5 ns was found in either ^{96}Rh or ^{97}Pd . However, the half-life of the $\frac{17}{2}^+$ level in ^{97}Pd has recently been determined¹⁷ to be between 2.0 and 2.5 ns. This empirical range is slightly slower than the value of 1.4 ns predicted by the shell-model calculation discussed later and corresponds to 1.3–1.7 W.u.

C. The Atomic masses of ^{96}Rh and ^{96}Pd

A recent evaluation of atomic masses¹⁸ lists the mass-excess values -86.073 ± 0.008 , -79.626 ± 0.013 , and -76.18 ± 0.15 MeV for ^{96}Ru , ^{96}Rh , and ^{96}Pd , respectively. The value for ^{96}Ru is obtained from a measurement¹⁹ of the mass difference between ^{96}Ru and C_7H_{12} molecules. The mass excess of ^{96}Rh is obtained from a measurement by Ashkenazi *et al.*²⁰ of the threshold beam energy for the $^{96}\text{Ru}(p,n)^{96}\text{Rh}$ reaction $E_{\text{th}} = 7.300 \pm 0.010$ MeV. This latter measurement was accomplished by recording

TABLE II. Transitions in ^{97}Pd produced by 167 MeV $^{40}\text{Ca} + ^{64}\text{Zn}$. The relative γ -ray intensities and angular distribution results are obtained from neutron-gated spectra and have been corrected for the efficiency and finite size of the detector. Several of the weaker transitions have been fitted by assuming that $A_4 = 0$. The $E2/M1$ mixing ratios δ are listed, using the phase convention of Yamazaki (Ref. 16), for three transitions.

E_γ (keV)	I_γ	A_2/A_0	A_4/A_0	Assignment
134.66(22)	2.7(3)	-0.18(27)	$\equiv 0$	$\frac{25}{2}^+ \rightarrow \frac{23}{2}^+$
170.70(18)	65.8(3.5) ^c	-0.29(3)	+0.00(6)	$\frac{21}{2}^+ \rightarrow \frac{19}{2}^+$ $-0.16 \leq \delta \leq -0.016$
184.03(22)	2.8(3)	-0.27(26)	$\equiv 0$	$\frac{31}{2} \rightarrow \frac{29}{2}^-$
224.85(22)	85.2(1.1)	-0.241(24)	-0.084(54)	$\frac{19}{2}^+ \rightarrow \frac{17}{2}^+$
227.66(30)	9.9(2.3) ^c	a	a	(6541 \rightarrow)
278.94(35)	1.3(6)	+0.7(12)	$\equiv 0$	4916 $\rightarrow \frac{29}{2}^+$
362.52(25)	80.4(3.9)	+0.32(6)	-0.20(6)	$\frac{17}{2}^+ \rightarrow \frac{13}{2}^+$
413.48(35)	2.7(9) ^c	a	a	2882 $\rightarrow \frac{19}{2}^+$
425.48(25)	12.5(2.6) ^c	-0.04(8) ^d	+0.11(17) ^d	($\rightarrow \frac{33}{2}^+$)
486.46(35)	4.2(1.6) ^c	a	a	($\rightarrow \frac{7}{2}^+$)
586.91(25)	102.7(1.6)	+0.241(43)	-0.084(88)	$\frac{13}{2}^+ \rightarrow \frac{9}{2}^+$
599.7 ^e	2.8(1.4) ^c	a	a	($\rightarrow \frac{13}{2}^+$)
608.32(30)	12.4(9)	-0.42(22) ^d	+0.33(39) ^d	$\frac{9}{2}^+ \rightarrow \frac{7}{2}^+$ $-7.0 \leq \delta \leq +0.037$
611.80(45)	8.4(9)	-0.30(24)	$\equiv 0$	$\frac{23}{2} \rightarrow \frac{21}{2}^+$
630.60(45)	3.1(8)	+0.07(62)	$\equiv 0$	1925 $\rightarrow \frac{9}{2}^+$
686.18(35)	31.7(2.2) ^d	+0.01(10) ^d	+0.10(18) ^d	$\frac{7}{2}^+ \rightarrow \frac{5}{2}^+$ $+0.048 \leq \delta \leq +0.34^f$
761.25(45)	4.0(1.4) ^c	a	a	3005 $\rightarrow \frac{17}{2}^+$
783.34(45)	7.0(1.0)	+0.06(31)	$\equiv 0$	1470 $\rightarrow \frac{7}{2}^+$
826.11(25)	58.1(3.4) ^c	+0.24(6) ^{b,d}	-0.08(9) ^{b,d}	$\frac{29}{2}^+ \rightarrow \frac{25}{2}^+$
898.99(45)	2.3(1.3)	-1.2(1.5)	$\equiv 0$	5536 $\rightarrow \frac{29}{2}^+$
944.37(45)	9.5(2.0) ^c	a	a	1631 $\rightarrow \frac{7}{2}^+$
981.97(35)	4.3(1.0) ^c	-0.98(28) ^d	$\equiv 0$	7523 \rightarrow 6541
1036.04(35)	5.2(1.3) ^c	a	a	$\frac{23}{2}^+ \rightarrow \frac{21}{2}^+$
1109.01(45)	7.2(8)	-0.58(27)	$\equiv 0$	$\frac{21}{2}^+ \rightarrow \frac{19}{2}^+$
1170.98(25)	58.0(3.4) ^c	+0.193(38) ^{b,d}	-0.062(81) ^{b,d}	$\frac{25}{2}^+ \rightarrow \frac{21}{2}^+$
1207.17(45)	10.0(9)	+0.06(5)	$\equiv 0$	$\frac{23}{2}^+ \rightarrow \frac{19}{2}^+$
1210.47(65)	weak	a	a	(\rightarrow 4916)
1250.99(25)	13.7(1.6) ^c	+0.28(17) ^d	+0.19(29) ^d	$\frac{33}{2}^+ \rightarrow \frac{29}{2}^+$
1294.54(22)	$\equiv 100.0(1.2)$	+0.247(34)	+0.073(76)	$\frac{9}{2}^+ \rightarrow \frac{5}{2}^+$
1541.71(45)	3.1(8)	-0.17(58)	$\equiv 0$	($\rightarrow \frac{21}{2}^+$)

^aTransition unresolved from another.

^bValue obtained from spectra recorded in singles mode.

^cValue obtained from γ - γ coincidence data.

^dValue may be perturbed by an unresolved transition.

^eEnergy adopted from ($^3\text{He}, 2n\gamma$) data.

^fThere is also a solution with $|\delta| > 1$.

excitation functions for four beta-delayed γ -ray transitions in the ^{96}Ru daughter nucleus. They also observed a prompt transition of 125 ± 2 keV with threshold beam energy of 7.425 ± 0.010 MeV. Therefore, this transition was attributed²⁰ to a decay to the ^{96}Rh ground state of a state at 125 keV excitation energy. The relative intensities of the four transitions that were produced in the ^{96}Ru daughter nucleus indicates that both of the beta-decaying isomers shown in Fig. 2 were being directly produced in the (p,n) experiment.²⁰ Although no quantitative information on the relative population of the two isomers was given, an inspection of their decay curve for the 832.6 keV $2^+ \rightarrow 0^+$ transition in ^{96}Ru indicates that the ^{96}Rh ground state was produced more intensely at a proton energy of 11 MeV.

Most recently, Rykaczewski *et al.*⁷ have studied the $\beta^+ + \text{EC}$ decay of ^{96}Pd to ^{96}Rh and have found a beta-decay Q value of 3.45 ± 0.15 MeV from a comparison of experimental and theoretical values for the ratio of intensities $\beta^+ / (\beta^+ + \text{EC})$. Moreover, they concluded⁷ that the (p,n) Q value measured by Ashkenazi *et al.*²⁰ refers instead to the 52.0 keV level of ^{96}Rh and accordingly adopted a mass excess for ^{96}Rh , which is 52.0 keV more bound than is listed in the compilation.¹⁸ Although they do not give the detailed reasoning for this conclusion, the observation by Ashkenazi *et al.*, mentioned earlier, that the threshold energy for a 125 ± 2 keV γ -ray is 125 keV higher than that for the ground state would have been decisive under the assumption that there is only one low-

lying transition in ^{96}Rh near 125 keV. However, as shown in Fig. 2, there are two transition energies in ^{96}Rh near 125 keV. It is probable that the one reported by Ashkenazi *et al.* is a mixture of both of these transitions with the $7^+ \rightarrow 6^+$ transition playing the dominant role. Then the tabulated value for ^{96}Rh mass excess¹⁸ would be nearly correct, although the binding energy may be underestimated by some fraction of 52.0 keV. The exact value of this fraction would depend on the relative population of the two isomers in the (p,n) data and on the detailed analysis of the excitation functions.²⁰ Therefore, adopting the tabulated mass excess for ^{96}Rh , the proposed mass excess of ^{96}Pd is -76.18 ± 0.15 MeV, in agreement with the tabulated value¹⁸ and 52 keV less bound than the value proposed by Rykaczewski *et al.*

D. Empirical systematics of the $N = 51$ nuclei

1. Odd- Z nuclei

It is worthwhile to compare the present results for ^{96}Rh with what has been found for the isotones ^{94}Tc and ^{92}Nb as shown in Fig. 4, where the $N = 51$ empirical levels are summarized across the proton $g_{9/2}$ shell from ^{91}Zr to ^{101}Sn . In both ^{92}Nb and ^{94}Tc , the complete multiplets $\pi g_{9/2} \times \nu d_{5/2}$ and $\pi p_{1/2} \times \nu d_{5/2}$ have been located. In addition, a 1^+ level at 442 keV in ^{94}Tc has been found. This level is populated in the $\beta^+ + \text{EC}$ decay of ^{94}Ru , with $\log ft = 3.9$, and has, therefore, a significant com-

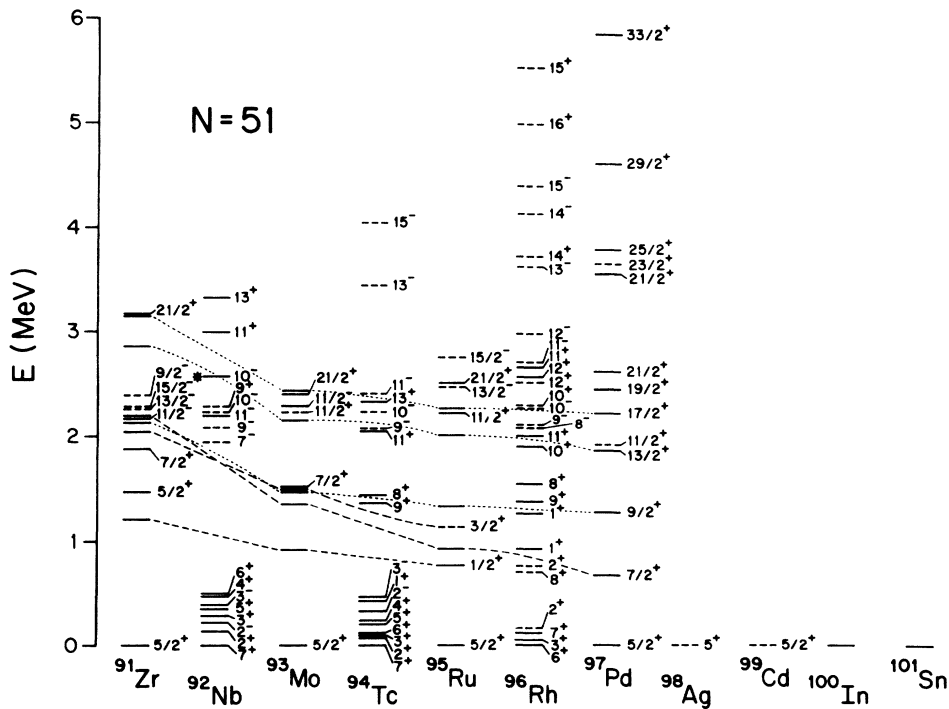


FIG. 4. The empirical yrast levels for the $N = 51$ system from the beginning of the $\pi g_{9/2}$ shell (^{91}Zr) to the end (^{101}Sn). Those levels whose spins or parities have only tentatively been assigned are shown as dashed. For the odd- A nuclei, those levels that are thought to have a large single-neutron component, either $\nu s_{1/2}$, $\nu d_{3/2}$, or $\nu g_{7/2}$, are connected by dashed lines. Moreover, the $\frac{9}{2}^+$, $\frac{13}{2}^+$, and $\frac{17}{2}^+$ levels, which involve the rearrangement of $g_{9/2}$ protons, are connected by dotted lines to guide the eye. The 10^- level in ^{92}Nb , which is marked with an asterisk was found using the (α, d) reaction (Ref. 26) and assigned the structure $\pi p_{1/2}^2 g_{9/2} \nu h_{11/2}$.

ponent of $\pi p_{1/2}^2 g_{9/2}^3 \nu g_{7/2}$. On the other hand, shell-model calculations^{21,22} have yielded a low-lying 1^+ level in ^{94}Tc , with the structure

$$\pi p_{1/2}^2 [g_{9/2}^3 (\nu=3)]_{7/2} \nu d_{5/2},$$

where the corresponding $\frac{7}{2}^+$ level has been found at 681 keV in ^{93}Tc . In ^{96}Rh , the positive-parity multiplet has been located, except for the 4^+ and 5^+ members, but not the negative-parity one.

The yrast 8^+ and 9^+ levels near 1.4 MeV in ^{94}Tc have been assigned the structure

$$[\pi g_{9/2} \times 2^+]_{11/2,13/2} \times \nu d_{5/2}$$

by Behar *et al.*¹⁴ and the corresponding yrast $\frac{11}{2}^+$ and $\frac{13}{2}^+$ levels have been found in ^{94}Tc . We propose an analogous structure for the 1392.8 and 1555.0 keV levels of ^{96}Rh shown in Fig. 2, where a corresponding yrast $\frac{13}{2}^+$ level has been found at 1351 keV in ^{95}Rh . In this regard, one anticipates the discovery in future experiments of an $\frac{11}{2}^+$ level in ^{95}Rh lying slightly above the $\frac{13}{2}^+$ level.

As mentioned in Sec. III A, the yrast 11^+ level in ^{96}Rh has the structure

$$\pi p_{1/2}^2 [g_{9/2}^5 (\nu=3)]_{17/2} \nu d_{5/2}$$

and is analogous to the yrast 11^+ level in ^{94}Tc . The yrast 12^+ level in ^{96}Rh has as yet no empirical analogue in ^{94}Tc . If the structure is

$$\pi p_{1/2}^2 [g_{9/2}^5 (\nu=3)]_{17/2} \nu g_{7/2},$$

then the 514.3 keV transition is of the type $\nu g_{7/2} \rightarrow \nu d_{5/2}$ and the positive A_2/A_0 value found for this transition indicates a positive $E2/M1$ mixing ratio (in the phase convention of Yamazaki¹⁶).

Behar *et al.*¹⁴ have found a 9^- level in ^{94}Tc at 2066 keV and assigned the structure

$$[\pi p_{1/2} g_{9/2}^4 (\nu=2)]_{13/2} \nu d_{5/2},$$

where the corresponding $\frac{13}{2}^-$ level has been found at 2145 keV in ^{93}Tc . We propose a similar structure for the yrast 9^- level in ^{96}Rh although a corresponding $\frac{13}{2}^-$ level has not yet been found in ^{95}Rh . The yrast 10^- level at 2235 keV in ^{94}Tc has been assigned the structure $\pi p_{1/2}^2 g_{9/2}^3 (\nu=1) \nu h_{11/2}$ by Behar *et al.* The 2289.2 keV yrast 10^- level in ^{96}Rh could receive a similar assignment. However, this latter level may contain significant admixtures of

$$[\pi p_{1/2} g_{9/2}^6 (\nu=2)]_{17/2} \nu d_{5/2}$$

or

$$[\pi p_{1/2} g_{9/2}^6 (\nu=2)]_{13/2} \nu g_{7/2}.$$

Moreover, the 10^- level in ^{94}Tc at 2235 keV was not populated strongly²³ in the (α, d) reaction at 50 MeV, but rather a level at 2.68 MeV was intensely produced. Therefore, this latter level is a more likely candidate to be the stretched $\pi g_{9/2} \nu h_{11/2}$ configuration than is the lower level found by Behar *et al.*

Each of the high-spin levels above 1.9 MeV in ^{92}Nb

shown in Fig. 4, except for the two 10^- levels, have been assigned²⁴ as the stretched configuration of a $d_{5/2}$ neutron to an empirical state of ^{91}Nb . The ^{91}Nb states in turn can be understood²⁵ as configurations of $\pi g_{9/2}^3$ or of $\pi p_{1/2} g_{9/2}^2$ outside of a ^{88}Sr core. The upper 10^- level at 2.58 MeV in ^{92}Nb was intensely produced²⁶ by the (α, d) reaction at 218 MeV and assigned to be the stretched $\pi g_{9/2} \nu h_{11/2}$ configuration. The lower 10^- level, on the other hand, was not populated strongly in this reaction at 218 MeV nor at 50 MeV (Ref. 23).

2. Even-Z nuclei

In Fig. 4, the excited states thought to have a significant single neutron component are connected by dashed lines for the $\nu g_{7/2}$, $\nu s_{1/2}$, and $\nu d_{3/2}$ orbitals. In addition, the ground states of ^{91}Zr , ^{93}Mo , ^{95}Ru , and ^{97}Pd correspond to the occupation of the $\nu d_{5/2}$ orbital. The structure assignments for these levels in both ^{91}Zr and ^{93}Mo are supported by (d, p) data, while the $\nu g_{7/2}$ assignments in both ^{93}Mo and ^{95}Ru are supported by the observation of beta-decay log ft values of about 5.1 to the levels ($\pi g_{9/2} \rightarrow \nu g_{7/2}$). The continuation of the $\nu g_{7/2}$ line to ^{97}Pd appears in Fig. 4 to be a reasonable extrapolation. Moreover, the yrast $\frac{9}{2}^+$, $\frac{13}{2}^+$, and $\frac{17}{2}^+$ levels are connected by dotted lines to guide the eye. These excitations involve the recoupling of $g_{9/2}$ protons and the energy spacings are similar to those found in the corresponding isotope with $N=50$, e.g., the $\frac{9}{2}^+ \rightarrow \frac{5}{2}^+$ transition energy in ^{91}Zr is 2132 keV, while the $2^+ \rightarrow 0^+$ transition energy in ^{90}Zr is 2186 keV.

E. Shell-model calculations

The mass region outside of the ^{88}Sr core has long been one of considerable interest to shell-model practitioners. There is a rich spectroscopy and there are relatively small model spaces that can be expected to be relevant. In recent years, heavy-ion reactions have enabled us to study nuclei farther from the stability line and there is now evidence that around ^{100}Zr there is a rather sudden transition from spherical to strongly deformed nuclei.²⁷ One can hope that with advancing shell-model and computer technology, one might have in this region a good opportunity to carry out credible shell-model calculations that could provide a quantitative description of the spectroscopy and show a transition from spherical to deformed behavior in one consistent microscopic model. The model space that has been used in the past²⁸ for spherical nuclei in this region assumes an inert ^{88}Sr core and works in an $n-p$ formalism. The $p_{1/2}$ and $g_{9/2}$ proton orbits have been treated as active orbits along with the $d_{5/2}$ and $s_{1/2}$ neutron orbits. In the calculations we discuss briefly here, we have extended the model space to include the $g_{7/2}$ neutron orbit. For the two nuclei under discussion in this paper, there are either seven or eight active protons. Some configurations thus will have either seven or eight protons in the $g_{9/2}$ orbit. The $n-p$ interaction is particularly strong between the $g_{7/2}$ neutron and the $g_{9/2}$ proton, and it is this strong $n-p$ interaction that is a major factor in the development of deformation.

This development is an ultimate aim of the shell-model calculation discussed in brief here. There is no similar strong n - p interaction for the $d_{3/2}$ neutron and the active proton orbits used here. We have made some calculations in a model space where the $d_{3/2}$ neutron orbit is active and find that the orbit has a negligible impact on the states studied here. We have therefore ignored the $d_{3/2}$ neutron orbit in all of the calculations discussed here. Given the assumption of this five-orbit model space, one must next specify the effective residual Hamiltonian. There are five single-particle energies, nine proton-proton (p - p) interaction matrix elements and 33 neutron-proton (n - p) interaction matrix elements. To determine these parameters, we proceeded as follows. We first determined the p - p matrix elements. The two proton single-particle energies and the nine p - p interaction matrix elements were fitted to 50 observed excitation energies of levels in the $N=50$ nuclei with $Z=39\rightarrow 44$. Quite analogous determinations of the p - p interaction have been made in the past.^{28,29} Suffice it to say that all of the observed low-lying states in the $N=50$ nuclei were well fitted. The observed levels with moderately high spins ($J^\pi=10^+$ and 11^-) in these nuclei in particular were in good agreement with experiment. Next, the n - p interaction was determined through the following steps. Since many of the nuclei treated here were originally treated in a four-orbit space where the $g_{7/2}$ neutron orbit was omitted, with considerable success, we first determined the n - p interaction in the four-orbit space. There are 14 n - p matrix elements in the four-orbit space. Ten of these were treated as free parameters and fitted to approximately 100 data points. Most of the levels are well fitted in this model space for $Z=39\rightarrow 46$. In fact there were only two states with firm experimental spin-parity assignments in the nuclei that we treated that could be called problem states in the smaller space, i.e., the second $J^\pi=\frac{7}{2}^+$ level in ^{91}Zr and the first $J^\pi=\frac{7}{2}^+$ level in ^{97}Pd . Thus the levels at low excitation in these nuclei could really at best determine two parameters of the effective Hamiltonian for the n - p interaction involving the $g_{7/2}$ orbit. The two most important parameters for this interaction are the $g_{7/2}$ single neutron energy and the center of gravity of the interaction between the $g_{9/2}$ proton and the $g_{7/2}$ neutron, i.e.,

$$\sum_J (2J+1) \langle \pi g_{9/2}, \nu g_{7/2} J | H_{pn} | \pi g_{9/2}, \nu g_{7/2} J \rangle .$$

In the present calculation of the $N=51$ nuclei, there is a Z -dependent effective single neutron energy which, in first approximation, yields a term $(Z-38)\times(\text{center of gravity})$. This term is thus of little importance in ^{91}Zr , but very important for ^{97}Pd . Thus, it is possible to fit the two "intruder" $J^\pi=\frac{7}{2}^+$ levels with these two neutron parameters. (It is worth noting that with the final set of parameters, the $d_{5/2}$, and $g_{7/2}$ levels are essentially degenerate in the single-particle spectrum of ^{101}Sn . This is consistent with the single-particle spectrum of ^{101}Sn used in shell-model calculations of the tin isotopes.³⁰) After these two parameters were adjusted, we found some sensitivity in the calculations to specific matrix elements of

the n - p interaction with the $g_{9/2}$ and $p_{1/2}$ proton orbits. In the final search, four of these specific matrix elements were treated as free parameters to be fitted to the observed spectra. In the final search, the p - p interaction was held fixed at the parameters determined by the $N=50$ nuclei and effectively 17 n - p interaction parameters were fitted to 100 observed levels in the $N=51$ nuclei with $Z=39\rightarrow 46$. Our primary purpose here is in the shell-model structure of ^{96}Rh and ^{97}Pd . Suffice it to say that there are no significant qualitative discrepancies for the spectrum of low-lying states in the $N=51$ nuclei with $Z=39\rightarrow 44$. We discuss first some of the details of the comparison of theory with experiment for ^{97}Pd . In Fig. 5 are plotted the yrast levels observed and calculated with the final effective interaction. This constructed experimental spectrum must be explained. Figure 5 indicates that the two levels near 2.5 MeV excitation have positive parity. If we assume positive parity for these levels, there is excellent agreement between calculation and experiment for all of the states below 3 MeV. There is only one $J^\pi=\frac{31}{2}^+$ state and no $\frac{33}{2}^+$ state in the model space. The observed position of a $\frac{33}{2}^+$ state indicates a definite breakdown of the model. We show in Fig. 5 the lowest two calculated levels for all spins allowed in the model space. There are calculated $J=\frac{1}{2}^+$ and $\frac{3}{2}^+$ levels at low excitation possibly not seen experimentally. If the primary

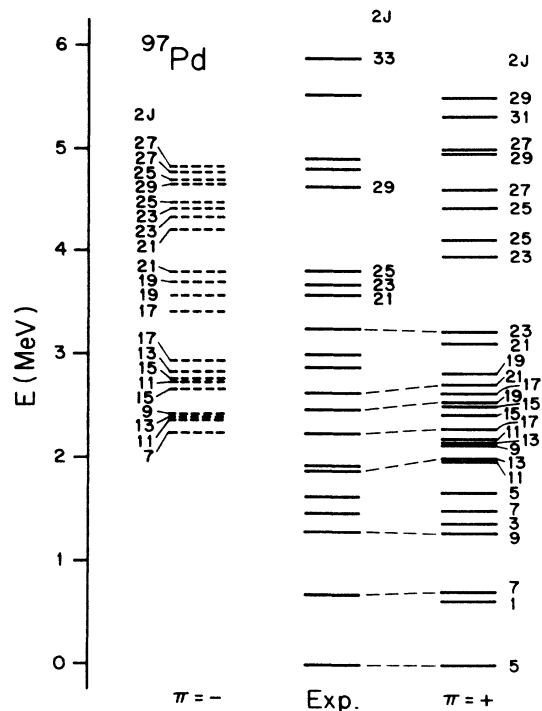


FIG. 5. Comparison of empirical yrast levels of ^{97}Pd with the results of shell-model calculations up to 6 MeV. The empirical levels are shown in the middle column. The right-hand column shows the lowest two positive-parity levels resulting from a calculation, while the calculated negative-parity levels are shown on the left. Positive- (negative-) parity levels are shown by solid (dashed) lines labeled on the right (left) with $2J$. Nine calculated nonyrast low-spin levels have been omitted for clarity.

feeding at low spins is through the yrast levels, these states would not be populated. Thus, in general, the simple shell model accounts for the low-lying states in ^{97}Pd quite well. We have calculated $E2$ and $M1$ rates for the low-lying states in ^{97}Pd . Bare $M1$ operator matrix elements were used and added effective charges of $0.5e$ were used to calculate the magnitude of $E2$ observables. There is an extremely strong calculated $B(M1) = 2 \mu_N^2$ between the $J^\pi = \frac{21}{2}^+$ and $\frac{19}{2}^+$ states near 2.5 MeV in the calculated spectrum. Using the theoretical B values and the observed energies of the transitions, the probability for a transition from the $\frac{21}{2}^+$ state to the $\frac{19}{2}^+$ state is favored by a factor of 10^5 over an $E2$ transition to the $\frac{17}{2}^+$ state. Thus, if the calculated numbers are approximately correct, it would be very difficult to see the stretched $E2$ transition. This does not eliminate all ambiguity, since the strong $B(M1)$ value for the decay of the lowest $J^\pi = \frac{21}{2}^+$ states in the lighter $N = 51$ nuclei is also found. In general then, the spherical picture for ^{97}Pd accounts rather well for the observed spectrum of states in ^{97}Pd .

In Fig. 6, the observed and calculated spectra for ^{96}Rh are shown. In the figure are shown all observed levels below 3 MeV excitation and the lowest two calculated states for all J values allowed in the model space. In the calculated spectrum, the lowest cluster of states results from coupling the $d_{5/2}$ neutron to the $(g_{9/2}^5, \nu = 1)$ proton configuration, with $J = 2 \rightarrow 7$. No $n-p$ interaction we found led to a $J = 9^+$ state below 1 MeV. Therefore, the calculations suggest that the state at 0.715 MeV is a $J^\pi = 8^+$ state. This assignment is consistent with the observed decay scheme. In the excitation energy range of 2.0 MeV and above there are numerous states with intermediate J values and there are reasonable analogs of all of the observed states in the calculated spectrum. Indeed this is true for all observed states up to 5.5 MeV excitation.

In summary, the spherical shell model reproduces many of the features of the measured spectra in both ^{96}Rh and ^{97}Pd . The overall $N = 51$ spectra calculations suggest that the $g_{7/2}$ neutron orbit is starting to be significant in ^{97}Pd . The data do not tell us much more than something about the appropriate single neutron energy for the $g_{7/2}$ orbit and the center of gravity of the $g_{7/2}-g_{9/2}$ $n-p$ interaction. There are a number of spectra known⁴ for the $N = 52$ nuclei in this mass region. Such data will provide some knowledge about the $n-n$ interaction and they may provide some more sensitivity to the remaining parts of the $n-p$ interaction.

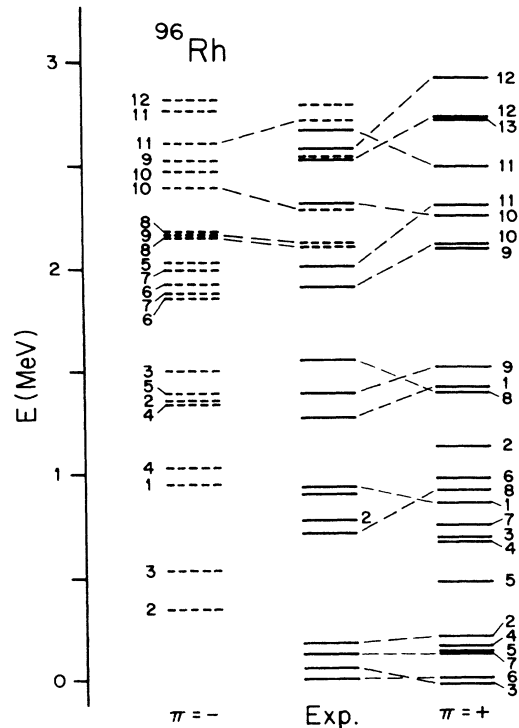


FIG. 6. Comparison of empirical yrast levels of ^{96}Rh up to 3 MeV, with the results of shell-model calculations. The empirical levels shown in the middle column are labeled on the right (left) with J for positive- (negative-) parity levels resulting from the calculation. The lowest two calculated levels of each spin-parity are shown, except that four calculated nonyrast low-spin levels have been omitted for clarity.

IV. CONCLUSIONS

To sum up, high-spin states of both ^{96}Rh and ^{97}Pd have been studied for the first time. The results have been utilized to determine the nuclear interaction in this mass region in the context of the shell model. The participation of the $g_{7/2}$ neutron was found to be significant for the first time in an $N = 51$ nucleus. It is anticipated that this orbital will be found in future experiments to play an even more important role in the spectra of the presently unstudied heavier $N = 51$ nuclides. Moreover, the spherical shell model was determined to be relevant to the interpretation of these nuclei. Finally, a consequence of a γ -ray doublet for the atomic masses of ^{96}Rh and ^{96}Pd was discussed.

¹W. F. Piel, Jr., G. Scharff-Goldhaber, C. J. Lister, and B. J. Varley, Phys. Rev. C **28**, 209 (1983).

²W. F. Piel, Jr. and G. Scharff-Goldhaber, Phys. Rev. C **30**, 902 (1984).

³W. F. Piel, Jr., G. Scharff-Goldhaber, C. J. Lister, and B. J. Varley, Phys. Rev. C **33**, 512 (1986).

⁴W. F. Piel, Jr., C. W. Beausang, D. B. Fossan, R. Ma, E. S. Paul, P. K. Weng, N. Xu, and G. Scharff-Goldhaber, Phys. Rev. C **37**, 1067 (1988).

⁵H. Grawe and H. Haas, Phys. Lett. **120B**, 63 (1983).

⁶D. Alber, H. Grawe, H. Haas, B. Spellmeyer, and X. Sun, Z. Phys. A **327**, 127 (1987).

⁷K. Rykaczewski, I. S. Grant, R. Kirchner, O. Klepper, V. T. Koslowsky, P. O. Larsson, E. Nolte, G. Nyman, E. Roeckl, D. Schardt, L. Spanier, P. Tidemand-Petersson, E. F. Zganjar, and J. Zylicz, Z. Phys. A **322**, 263 (1985).

⁸P. Fettweis, P. Del Marmol, M. Degreef, P. Duhamel, and J. Vanhorenbeeck, Z. Phys. A **305**, 57 (1982).

- ⁹W. F. Piel, Jr., G. Scharff-Goldhaber, C. J. Lister, and B. J. Varley, *Bull. Amer. Phys. Soc.* **28**, 686 (1983).
- ¹⁰T. A. Walkiewicz, S. Raman, and J. B. McGrory, *Phys. Rev. C* **27**, 1710 (1983).
- ¹¹L. Hildingsson, C. W. Beausang, D. B. Fossan, W. F. Piel, Jr., A. P. Byrne, and G. D. Dracoulis, *Nucl. Instrum. Methods* **A252**, 91 (1986).
- ¹²S. C. Gujrathi, C. Weiffenbach, and J. K. P. Lee, *J. Phys. G (London)* **1**, 67 (1975).
- ¹³F. Rosel, H. M. Fries, K. Alder, and H. C. Pauli, *At. Data Nucl. Data Tables* **21**, 91 (1978).
- ¹⁴M. Behar, A. Ferrero, A. Filevich, G. Garcia-Bermudez, and M. A. J. Mariscotti, *Nucl. Phys.* **A373**, 483 (1982).
- ¹⁵E. Nolte, G. Korschinek, and U. Heim, *Z. Phys. A* **298**, 191 (1980).
- ¹⁶T. Yamazaki, *Nucl. Data Sect. A* **3**, 1 (1967).
- ¹⁷D. Alber, H. Grawe, H. H. Bertschat, H. Haas, B. Spellmeyer and X. Sun, (to be published).
- ¹⁸A. H. Wapstra, G. Audi, and R. Hoekstra, *At. Data Nucl. Data Tables* **39**, 281 (1988).
- ¹⁹R. A. Damerow, R. R. Ries, and W. H. Johnson, Jr., *Phys. Rev.* **132**, 1673 (1963).
- ²⁰J. Ashkenazi, E. Friedman, D. Nir, and J. Zioni, *Nucl. Phys.* **A158**, 146 (1970).
- ²¹K. H. Bhatt and J. B. Ball, *Nucl. Phys.* **63**, 286 (1965).
- ²²J. Vervier, *Nucl. Phys.* **75**, 17 (1966).
- ²³M. S. Zisman and B. G. Harvey, *Phys. Rev. C* **5**, 1031 (1972).
- ²⁴B. A. Brown and D. B. Fossan, *Phys. Rev. C* **15**, 2044 (1977).
- ²⁵B. A. Brown, P. M. S. Lesser, and D. B. Fossan, *Phys. Rev. C* **13**, 1900 (1976).
- ²⁶H. Langevin-Joliot, V. Datar, E. Gerlic, J. Van de Wiele, F. Azaiez, S. Fortier, S. Gales, J. Guillot, J. M. Maison, C. P. Massolo, G. Duhamel, and G. Perrin, *Phys. Rev. C* **38**, 1168 (1988).
- ²⁷P. Federman and S. Pittel, *Phys. Rev. C* **20**, 820 (1979).
- ²⁸K. H. Bhatt and J. B. Ball, *Nucl. Phys.* **63**, 286 (1965); S. Cohen, R. D. Lawson, M. H. MacFarlane, and M. Soga, *Phys. Lett.* **10**, 195 (1964); J. B. Ball, J. B. McGrory, and J. S. Larsen, *Phys. Lett. B* **41**, 581 (1972).
- ²⁹F. J. D. Serduke, R. D. Lawson, and D. N. Gloeckner, *Nucl. Phys.* **A256**, 45 (1976).
- ³⁰H. Prade, W. Enghardt, W. D. Fromm, H. U. Jager, L. Kaubler, H. J. Keller, L. K. Kostov, F. Sary, G. Winkler, and L. Westerberg, *Nucl. Phys.* **A425**, 317 (1984).